Phase Transformations of Fe_3N–Fe_4N Iron Nitrides at Pressures up to 30 GPa Studied by In Situ X-ray Diffractometry

K. D. Litasov[a, b], A. F. Shatskiy[a, b], S. G. Ovchinnikov[c, d], Z. I. Popov[d], D. S. Ponomarev[b], and E. Ohtani[e]

[a] *Sobolev Institute of Geology and Mineralogy, Siberian Branch, Russian Academy of Sciences, pr. Akademika Koptyuga 3, Novosibirsk, 630090 Russia*
e-mail: klitasov@igm.nsc.ru
[b] *Novosibirsk State University, ul. Pirogova 2, Novosibirsk, 630090 Russia*
[c] *Kirensky Institute of Physics, Siberian Branch, Russian Academy of Sciences, Akademgorodok, Krasnoyarsk, 660036 Russia*
[d] *Siberian Federal University, Krasnoyarsk, 660041 Russia*
[e] *Department of Earth and Planetary Materials Science, Graduate School of Science, Tohoku University, Sendai 980-8578, Japan*
Received October 28, 2013

The parameters of the equation of state of the stable ε-Fe_3N_x (where $x = 0.8$) nitride in the Fe–N system have been determined at pressures up to 30 GPa and temperatures up to 1273 K. The parameters $V_0 = 81.48(2)$ Å^3, $K_T = 162(3)$ GPa, $K_T = 4.0 = 1.66(2)$, $\gamma_0 = 555$ K, and $q = 1$ have been determined for ε-$Fe_3N_{0.8}$ by the approximation of the P–V–T data with the Vinet equation of state and the thermal parameters within the Mie–Grüneisen–Debye formalism. No anomalous change in the volume of the cell owing to possible magnetic transitions has been revealed. The instability of Fe_4N at high pressures and Fe_3N in the presence of a deficit of nitrogen in the system has been established. The stable phase in the temperature range of 300–673 K and the pressure range of 20–30 GPa is ε-Fe_3N rather than ε-$Fe_3N_{0.8}$.

DOI: 10.1134/S0021364013250140

High-strength iron nitrides are of interest as wear-resistant materials with increased fatigue and corrosion resistance [1, 2]. They have strong magnetic properties (the magnetic moment of Fe_4N is 2.0–2.7 μ_B). Accordingly, the relation between the chemical bond and magnetism was studied in numerous works [3, 4]. Furthermore, study of stability and thermoelastic properties of iron nitrides is of significant importance for geophysics because they can be a component of the inner and outer (in the content of a liquid) core of the Earth [5]. Nitrogen is one of the least studied elements in the composition of the Earth. Its content in the inner shells, including the core, remains hardly known [6].

The Fe–N system at a pressure of 0.1 MPa contains a number of intermediate compounds varying from γ-Fe_4N (roaldite) to ζ-Fe_2N and intermediate nitride ε-Fe_3N_x with a series of isostructural nonstoichiometric compounds with $x = 0.75$–1.4 [7, 8]. The stoichiometric ε-Fe_3N compound most likely has the symmetry $P6_322$. However, most other ε-Fe_3N_x compounds have the space group $P312$. The temperature dependence of the composition ε-Fe_3N_x complicates analysis of the equation of state and elastic properties of this nitride.

Iron nitrides have been intensively studied in recent years in experiments at high pressures and temperatures. Upon heating in a multianvil press, synthesis of ε-Fe_3N_x from γ-Fe_4N occurs at 8.5(8) GPa and 1373(150) K [9], as well as at 15(2) GPa and 1600(200) K [10]. The parameters of the equation of state of γ-Fe_4N, ε-$Fe_3N_{1.05}$, and ε-Fe_7N_3 compressed in a diamond anvil cell were found [5, 9, 11]. It was found that the compression of γ-Fe_4N in the diamond anvil cell at 298 K leads to the spontaneous formation of ε-$Fe_3N_{0.75}$ at a pressure above 17 GPa. However, the boundary of the transition is kinetic and the complete transformation was not observed upon further compression even to 33 GPa [9, 12]. The elastic properties, the equations of state, and the electronic structure of iron nitrides were theoretically studied in [9–11, 13, 14].

The aim of this work is to obtain iron nitrides in experiments at pressures up to 30 GPa and to systematically study their thermoelastic properties, which
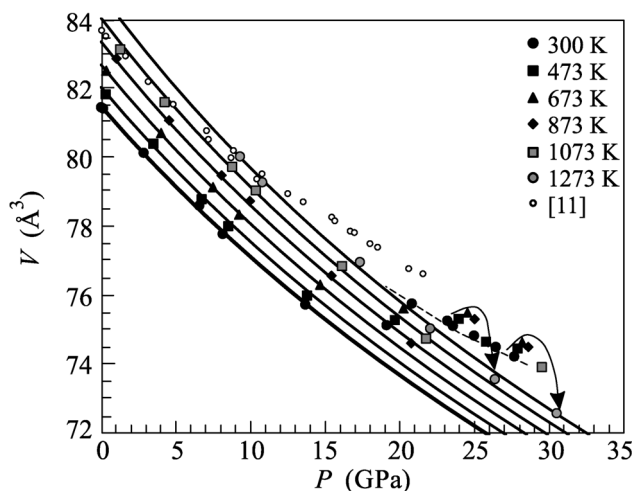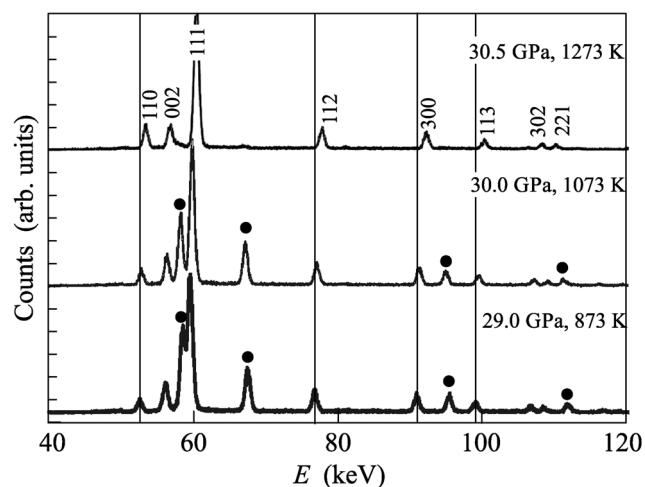
Fig. 1. Approximation of the $P-V-T$ data for ε-Fe$_3$N$_x$ with the Mie−Grüneisen−Debye equation of state. The points are the experimental data and the solid lines are the corresponding calculated isotherms. The dashed line is change in the volume of ε-Fe$_3$N$_x$ at 298 K and pressures above 20 GPa. The arrows show changes in the volume with an increase in the temperature in the first two heating cycles.

Fig. 2. Diffraction patterns of iron nitrides at 30 GPa. The peaks of ε-Fe$_3$N$_x$ are marked according to space group P312. The closed circles indicate the peaks of γ-F$_4$N. It can be seen that peaks of ε-Fe$_3$N$_x$ are shifted toward lower energies (smaller volume of the cell) with an increase in the temperature.

were previously studied for a number of compounds only at room temperature.

To this end, an experiment with several cycles of heating of a sample with in situ X-ray diffractometry involving synchrotron radiation was performed at the BL04B1 station of the SPring-8 facility (Japan), where two Kawai-type multianvil hydraulic presses are installed. We used a standard configuration of a high-pressure cell based on zirconium and magnesium oxides placed in an octahedral cavity in the center of a unit of eight WC anvils with a truncation edge length of 2 mm. A lanthanum chromite was used to heat the cell. A capsule was made of BN. The temperature was measured by means of a W−Re (3/25%) thermocouple. The characteristics of various cells and the method of synchrotron experiments were considered in detail in [15–17]. A sample consisting of a mixture of ε-Fe$_3$N and γ-Fe$_4$N was placed in the capsule in order to determine the cell parameters of both nitrides. The sample was separated by a BN plate from a pressure marker, which consisted of a mixture of MgO and Au, at the equivalent position with respect to the heater. The pressure was determined in terms of the volume of the unit cell of the reference with the use of the equation of state from [18]. To determine the unit cell parameters, we used eight or nine peaks for space group P312.

The experimental results are shown in Fig. 1, where the compression curve of the nitride at 300 K in the pressure range of 1−17 GPa is inconsistent with that in the pressure range of 17−30 GPa. Points above 30 GPa are close to the continuation of the compression curve for ε-Fe$_3$N$_{1.05}$ from [11]. There is an additional char-

acteristic feature. The points of volumes at a temperature of 1273 K and pressures of 17−30 GPa lie on the continuation of the compressibility isotherm at lower pressures, and the volume of the unit cell in the first three heating cycles (beginning with high pressures) first increases in the range of 300 to 673 K and then decreases in the range of 873−1273 K. This behavior of ε-Fe$_3$N$_x$ corresponds to a decrease in x with an increase in the temperature, which is similar to the behavior of the ε nitride on the phase diagram of Fe−N at 0.1 MPa. This change in the volume is additionally accompanied by the complete disappearance of γ-Fe$_4$N on the diffraction pattern at 1273 K (Fig. 2).

Consistency of the points of ε-Fe$_3$N$_x$ on the $P-V-T$ diagram (Fig. 1) indicates that change in the composition of the phase with a further heating to a moderate temperature of 1273 K was insignificant. The unit cell parameters of ε-Fe$_3$N$_x$ calculated after the experiment are $a = 4.6461(2)$ Å, $b = 4.3566(2)$ Å, and $V = 81.44(1)$ Å^3. Using a linear dependence of the composition of ε nitrides on the volume of the unit cell [9, 12], we obtain $x = 0.80$. The composition of the nitride was also measured by the electron-probe analysis with the use of a Tescan MYRA 3 LMU instrument with an energy dispersion attachment. Chromium deposition was used in the analysis. The signal from nitrogen was calibrated with the use of the Fe$_3$N and Fe$_4$N references. The measured composition was closed to the calculated one with $x = 0.78 \pm 0.05$. Peaks of boron and oxygen were not observed. Thus, the composition of the nitride for which the equation of

Thermoelastic parameters of iron nitrides

	Method	P, GPa	V_0, Å^3	K_T, GPa	K_T'	References
ε-Fe$_3$N$_{0.8}$	MA	0–31	81.48(2)	162(3)	**4.0**	This work
ε-Fe$_3$N$_{1.1}$	DAC	0–10	84.77	172	**5.7**	[11]
ε-Fe$_3$N	DFT		81.00	214		[11]
ε-Fe$_3$N	DFT		82.83	170.9		[14]
ε-Fe$_3$N	DFT		83.55	191.5		[13]
ε-Fe$_7$N$_3$	DAC	0–51	86.04	168	5.7	[5]
γ-Fe$_4$N	DAC	0–33	54.50	155.8	4.23	[9]
γ-Fe$_4$N	DAC	0–31	54.95	155	**4.0**	[5]
γ-Fe$_4$N	DFT			166	4.24	[10]
γ-Fe$_4$N	DFT		54.64	191.8		[20]

Fixed values are given in bold. The thermal parameters are $\gamma_0 = 1.66$ at the fixed parameter $q = 1$ and $\theta_0 = 555$ K [14]; $\partial K_T/\partial T = -0.019(2)$ GPa/K, $a = 3.76(14)$ K^{-1}, $b = 0.35(18)$ K^{-2} ($\alpha = a + bT$); MA means the multianvil press, DAC stands for the diamond anvil cell, and DFT means the density functional theory (see references for details of the calculations)

state was obtained is ε-Fe$_3$N$_{0.8}$. This nitride is likely close to ε-Fe$_3$N$_{0.75}$ studied in [9].

The $P–V–T$ data for ε-Fe$_3$N$_{0.8}$ at 298 K were approximated with the third-order Vinet equation of state $P = [3K_T(1 - y)/y^2]\exp[1.5(K_T' - 1)(1 - y)]$, where $y = (V/V_0)^{1/3}$. Two standard equations of state—Mie–Grüneisen–Debye and high-temperature—were used at high temperatures. The formalism of the calculations with these equations of state was presented, e.g., in [17, 19]. The $P–V–T$ data were processed with the OriginPro 8.0 program. Each method involves six parameters for the least squares optimization. In the case of the Mie–Grüneisen–Debye equation of state, these are the volume V_0 of the unit cell at 0.1 MPa and 298 K, isothermal bulk modulus K_T, its derivative with respect to the pressure $K_T' = \partial K_T/\partial P$, the Grüneisen parameter γ_0, Debye temperature θ_0, and the dimensionless parameter q. In the case of the high-temperature equation of state, these are V_0, K_T, K_T', the derivative of K_T with respect to the temperature ($\partial K_T/\partial T$), and the thermal expansion $\alpha = a_1 + a_2 T$.

The table presents the thermoelastic parameters obtained for ε-Fe$_3$N$_{0.8}$ in comparison with the literature data for iron nitrides. The values of V_0, K_T, and K_T' were obtained by approximating the 298 K isotherm. Since the data are limited in pressure (13 GPa), a value of 4 is taken for the derivative K_T'. The found K value appeared to be smaller than the values obtained in previous experiments and calculated theoretically for ε-Fe$_3$N$_x$. The calculated isotherms for the Mie–Grüneisen–Debye equation of state are in good agreement with the experimental data (Fig. 1), although the approximation was performed at a fixed Debye temperature (555 K [14]) and parameter q. The Grüneisen thermal parameter ($\gamma = 1.66$) hardly depends on the parameter q (the calculated value is $q = 0.18$). The

thermal expansion of ε-Fe$_3$N$_x$ calculated from our data at high pressure is shown in Fig. 3 in comparison with preceding measurements at 0.1 MPa. Pronounced correlation of an increase in the thermal expansion with an increase in the content of nitrogen in the nitride is observed.

According to the previous experiments, the stability field of ε-Fe$_3$N$_{0.8}$ at low pressures (1–5 GPa) is limited by a temperature of 1173 K. However, greater heating is not accompanied by the transition to Fe$_4$N, which is observed for ε-Fe$_3$N$_{0.75}$ at 525 K and 0.1 MPa [9].

It was revealed in the previous studies that the content of nitrogen in ε-Fe$_3$N$_x$ significantly affects the electronic configuration of iron atoms and their magnetic properties. With an increase in the content of nitrogen from $x = 1$ to $x = 1.48$, the Curie temperature T_C and saturation magnetization M_S decrease monotonically (from 575 to ~300 K and from 2.1 to 1.2 μV, respectively [12]). However, the magnetization of ε-
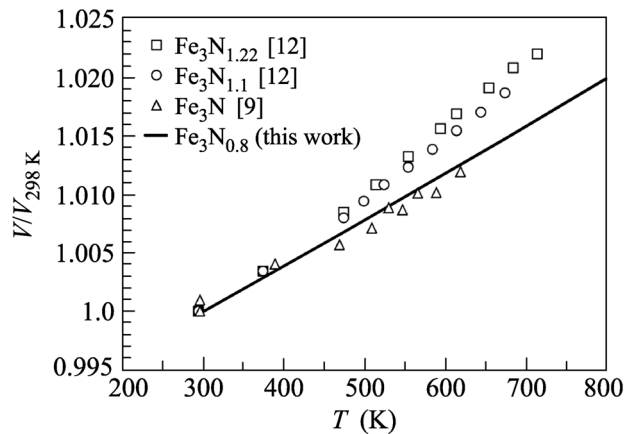

Fig. 3. Temperature dependence of the volume of ε-Fe$_3$N$_x$ at 0.1 MPa, indicating the difference in thermal expansion depending on the content of nitrogen in nitride.

$Fe_3N_{0.75}$ hardly differs from that for ε-Fe_3N. The authors of [9] attributed this property to the compensation effect of an increased magnetization of iron atoms with a low coordination number. The theoretical density functional calculation shows a decrease in the magnetic moment from 2.1 μV for ε-Fe_3N to 1.9 μV for ε-$Fe_3N_{0.75}$. However, compensating atoms (with one and zero neighboring nitrogen atoms) have a magnetic moment of 2.3–2.7 μV [9]. In contrast to other iron compounds, the transition from the ferromagnetic to paramagnetic form of ε-Fe_3N_x occurs without a significant change in the unit cell parameters (see Fig. 3). For this reason, we could not determine the possible parameters of magnetic transitions at high pressure by X-ray diffractometry.

Thus, data on the $P-V-T$ equation of state of the iron nitride stable at high pressures and temperatures have been obtained for the first time. We have studied the ε-$Fe_3N_{0.8}$ nitride synthesized at 30 GPa and 1473 K. The high-temperature measurements generally demonstrate lower compression moduli than the experiments in a diamond anvil cell at 300 K and theoretical estimates for 0 K.

The stability boundaries of various iron nitrides at a pressure of about 20 GPa should be more reliably determined in future experiments. In addition, for a more complete thermodynamic description [17, 21] of new high-pressure iron nitrides, their thermal chemistry at 0.1 MPa should be investigated. It is noteworthy that the Fe–N system is the most complicated for study at high pressures as compared to other iron-bearing systems concerning the Earth's core. The experimental results on iron nitrides at pressures below 30 GPa can hardly be extrapolated to pressures of 340–360 GPa in the solid inner core of the Earth. For this reason, additional studies in diamond anvil cells are necessary for estimation of the maximum content of nitrogen in the Earth's core. It is important to study both the $P-V-T$ equation of state and magnetic transitions [22, 23].

REFERENCES

1. H. Jacobs, D. Rechenbach, and U. Zachwieja, J. All. Comp. **227**, 10 (1995).

2. N. I. Kardonina, A. S. Yurovskikh, and A. S. Kolpakov, Metalloved. Term. Obrab. Met. **10**, 5 (2010).

3. B. Eck, R. Dronskowski, M. Takahashi, and S. Kikkawa, J. Mater. Chem. **9**, 1527 (1999).

4. M. Sifkovits, H. Smolinski, S. Hellwig, and W. Weber, J. Magn. Magn. Mater. **204**, 191 (1999).

5. J. F. Adler and Q. Williams, J. Geophys. Res.: Solid Earth **110**, BO1203 (2005).

6. W. F. McDonough, in *Treatise on Geochemistry*, Ed. by H. D. Holland and K. K. Turekian (Elsevier, Pergamon, Oxford, 2003), Vol. 2, p. 547.

7. K. H. Jack, Proc. R. Soc. London A **208**, 200 (1951).

8. H. A. Wriedt, N. A. Gokcen, and R. H. Nafziger, Bull. Alloy Phase Diagr. **8**, 355 (1987).

9. K. Guo, D. Rau, J. von Appen, Y. Prots, W. Schnelle, R. Dronskowski, R. Niewa, and U. Schwarz, High Press. Res. **33**, 684 (2013).

10. R. Niewa, D. Rau, A. Wosylus, K. Meier, M. Wessel, M. Hanfland, R. Dronskowski, and U. Schwarz, J. Alloys Comp. **480**, 76 (2009).

11. R. Niewa, D. Rau, A. Wosylus, K. Meier, M. Hanfland, M. Wessel, R. Dronskowski, D. A. Dzivenko, R. Riedel, and U. Schwarz, Chem. Mater. **21**, 392 (2009).

12. A. Leineweber, H. Jacobs, F. Huning, H. Lueken, and W. Kockelmann, J. Alloys Comp. **316**, 21 (2001).

13. Y.-J. Shi, Y.-L. Du, and G. Chen, Comp. Mater. Sci. **67**, 341 (2013).

14. W. Zhang, Z. Lv, Z. Shi, S. Sun, Z. Wang, and W. Fu, J. Magn. Magn. Mater. **324**, 2271 (2012).

15. A. Shatskiy, T. Katsura, K. D. Litasov, A. V. Shcherbakova, Y. M. Borzdov, D. Yamazaki, A. Yoneda, E. Ohtani, and E. Ito, Phys. Earth Planet. Int. **189**, 92 (2011).

16. K. D. Litasov, A. Shatskiy, Y. Fei, A. Suzuki, E. Ohtani, and K. Funakoshi, J. Appl. Phys. **108**, 053512 (2010).

17. K. D. Litasov, P. I. Dorogokupets, E. Ohtani, Y. Fei, A. Shatskiy, I. S. Sharygin, P. N. Gavryushkin, S. V. Rashchenko, Y. V. Seryotkin, Y. Higo, K. Funakoshi, A. D. Chanyshev, and S. S. Lobanov, J. Appl. Phys. **113**, 093507 (2013).

18. T. S. Sokolova, P. I. Dorogokupets, and K. D. Litasov, Geol. Geofiz. **54**, 237 (2013).

19. K. D. Litasov, E. Ohtani, S. Ghosh, Y. Nishihara, A. Suzuki, and K. Funakoshi, Phys. Earth Planet. Int. **164**, 142 (2007).

20. T. Gressmann, M. Wohlschlögel, S. Shang, U. Welzel, A. Leineweber, E. J. Mittemeijer, and Z. K. Liu, Acta Mater. **55**, 5833 (2007).

21. K. D. Litasov, I. S. Sharygin, P. I. Dorogokupets, A. Shatskiy, P. N. Gavryushkin, T. S. Sokolova, E. Ohtani, J. Li, and K. Funakoshi, J. Geophys. Res.: Solid Earth **2013**, JB010270 (2013).

22. I. S. Lyubutin, V. V. Struzhkin, A. Mironovich, A. G. Gavriliuk, P. G. Naumov, J.-F. Lin, S. G. Ovchinnikov, S. Sinogeikin, P. Chow, and Y. Xiao, Proc. Natl. Acad. Sci. **110**, 7142 (2013).

23. I. S. Lyubutin and A. G. Gavrilyuk, Phys. Usp. **52**, 989 (2009).

Translated by R. Tyapaev